BEAM PHYSICS CHALLENGES IN RAON*

Ji-Ho Jang, Dong-O Jeon#, Hyojae Jang, Hyung Jin Kim, Ilkyoung Shin, IBS, Daejeon, Korea
Ji-Gwang Hwang, Eun-San Kim, KNU, Daegu, Korea

Abstract

Construction of the RAON heavy ion accelerator facility is under way in Korea. As high intensity 400 kW superconducting linac (SCL) is employed as a driver, beam physics aspects are carefully studied. The SCL is based on lattice consisting of cryomodules and quadrupole doublets. Beam dynamics studies for the RAON has progressed to cover start-to-end simulations and machine imperfection studies confirming beam loss less than 1 W/m. At present, prototyping of major components are proceeding including 28 GHz ECR ion source, RFQ, superconducting cavities, magnets and cryomodules. First article of prototype superconducting cavities have been delivered that were fabricated through domestic vendors. Prototype HTS quadrupole is under development. Progress report of the RAON accelerator systems is presented.

INTRODUCTION

The RISP (Rare Isotope Science Project) is developing a heavy ion accelerator called RAON, and experimental facilities. One of the characteristics of RAON facility is that it will be able to supply RI beams with both IF (In-flight Fragmentation) and ISOL (Isotope Separator On-Line) methods [1,2]. The layout of the facility is given in Fig. 1.

The RAON consists of a driver linac and a post linear accelerator. The driver linac includes an injector of an ECR ion source, an RFQ, and a SCL (superconducting linac) called SCL1 and SCL2 which are separated by a 90° charge selection section. It can accelerate uranium beams up to 200 MeV/u and proton beams up to 600 MeV as summarized in Table 1. The stable ion beams with beam power up to 400 kW are delivered to the IF target and various experimental areas. The post linac is used to accelerate RI beams which are generated by the ISOL facility. A cyclotron delivers 1 mA 70 MeV proton beams to the ISOL target. The cyclotron has dual extraction ports with thin carbon foils for charge exchange extraction of H^- beam. The rare isotope beams generated by the ISOL system is accelerated by a chain of post accelerators including RFQ and another superconducting linac, SCL3. The RI beams can be delivered into the low energy experimental hall or can be injected through P2DT to the SCL2 in order to accelerate to higher energy.

Construction of the RAON heavy ion accelerator facility started on December 2011. The design of the accelerator systems has progressed, and prototyping of critical components and systems have been materialized. In this paper, the status of the RAON accelerator systems is presented along with beam dynamics design and prototyping progress.

*Work supported by Ministry of Science, ICT and Future Planning
#jeond@ibs.re.kr

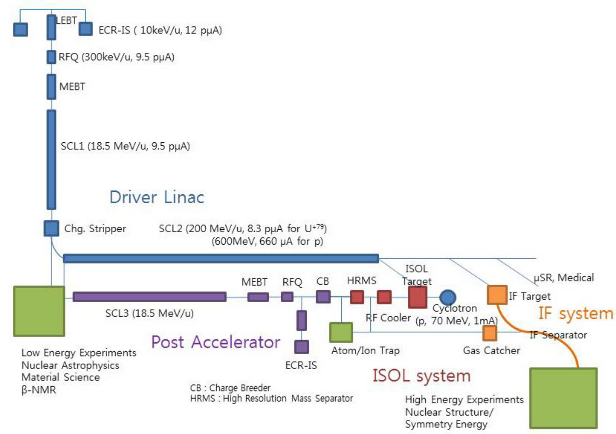

Figure 1: Layout of RAON Linac.

Table 1: Beam Specification for the Driver Linac

Parameters	H^+	O^{8+}	Xe^{54+}	U^{79+}
Energy [MeV/u]	600	320	251	200
Current [pμA]	660	78	11	8.3
Power on target [kW]	>400	400	400	400

DRIVER LINAC

Injector

The injector of RAON driver linac consists of a 28 GHz ECR ion source, an LEBT (Low Energy Beam Transport), a 500 keV/u RFQ (Radio-Frequency Quadrupole), and a MEBT (Medium Energy Beam Transport) [1, 3].

The two-charge-state (33 and 34) uranium beams are injected into the RFQ in order to achieve the required beam power of 400 kW at the IF target. The electrostatic quadrupoles are used to focus the two charge state beams. We considered a multi-harmonic buncher and a velocity equalizer for reducing the longitudinal rms beam emittance. The beam envelope in the LEBT is shown in

ISBN 978-3-95450-173-1

Fig. 2 which is calculated by TRACK code [4].

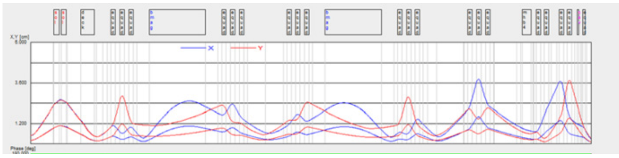

Figure 2: Beam envelope in the LEBT.

The RFQ accelerates the stable ion beams from 10 keV/u to 500 keV/u. The 81.25 MHz RFQ operates in CW mode. The design parameters are summarized in Table 2. Figure 3 shows the PARMTEQ simulation results [5]. The transmission rate becomes more than 98% and the total length is about 5 m.

Table 2: RAON RFQ Specifications

Parameters	Value
Particles	Proton to $^{238}U^{33+,34+}$
Frequency	81.25 MHz
Input / Output Energy	10 keV/u / 500 keV/u
Transmission	98%
Peak Surface Field	1.7 Kilpatrick
Operation Mode	CW
Length	4.94 m

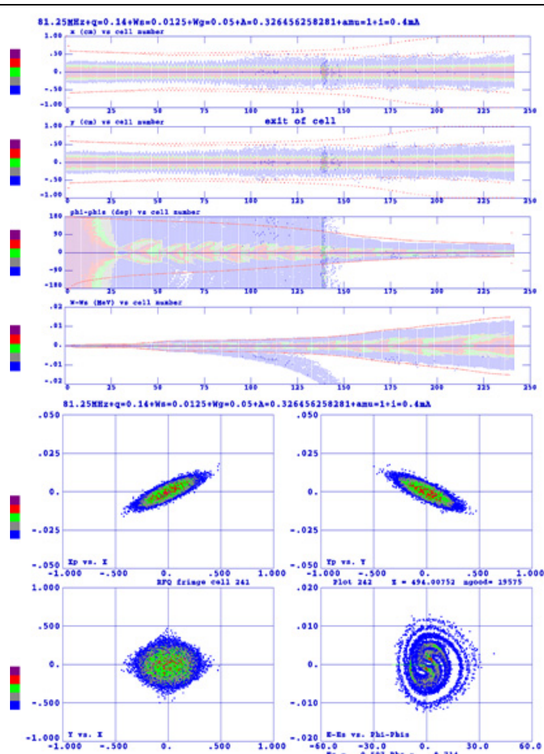

Figure 3: PARMTEQ simulation result of the RFQ.

The MEBT consists of 3 buncher cavities and 8 quadrupole magnets for longitudinal and transverse beam manipulations [1, 6]. The TRACK simulation results are given in Fig. 4 for the beam envelope and particle distributions in transverse phase spaces.

The prototype ECR ion source and the prototype RFQ of one section are finished as shown in Fig. 5 and Fig. 6. The low temperature test of the assembled superconducting magnet is in progress for the ECR ion source. The RF test of the RFQ prototype is also going on.

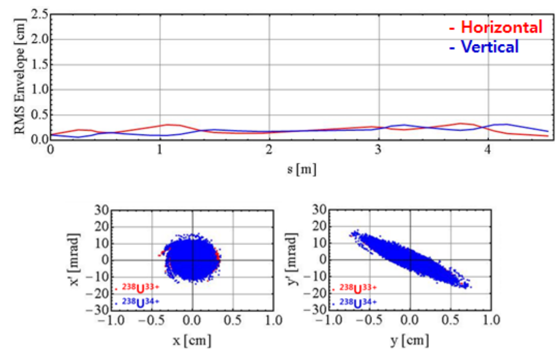

Figure 4: RMS beam envelope in RAON MEBT (upper plot) and particle distribution at the entrance of SCL (lower plot).

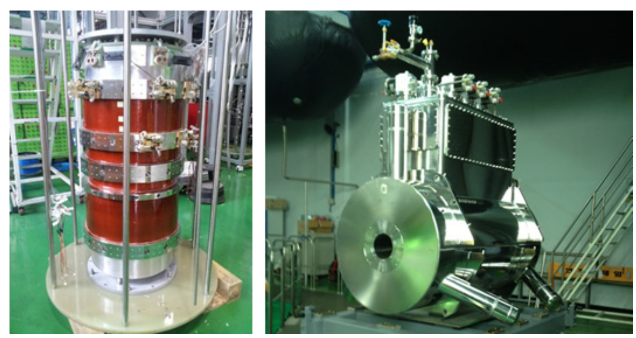

Figure 5: Assembled ECR superconducting magnet (left) and fabricated cryostat (right) of ECR ion source.

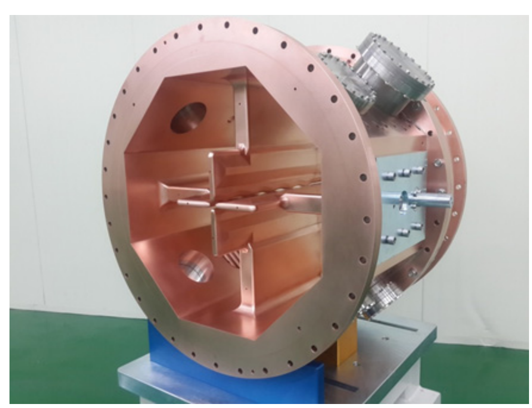

Figure 6: Fabricated RFQ prototype.

ISBN 978-3-95450-173-1

Superconducting Linac

The SCL of RAON driver linac consists of a low energy part of SCL1, a CSS (Charge Selection Section) and a high energy part of SCL2 [1, 7]. SCL1 uses two different type of cavities, QWR (Quarter Wave Resonator) and HWR (Half Wave Resonator), in order to accelerate uranium beams up to around 18 MeV/u. The charge stripper in CSS generates higher charge states of around 79 for the uranium beams. The CSS selects 5 charge states from 77 to 81. SCL2 uses two different type of SSR (Single Spoke Resonator) cavities, SSR1 and SSR2, in order to accelerate beams up to 200 MeV/u. The design parameters of the RAON superconducting cavities are summarized in Table 3 [7]. The energy gain in each type of cavities is given in Fig. 7 [1]. The required number of cryomodules and cavities are summarized in Table 4.

Table 3: RAON Superconducting Cavity Parameters

Parameters	Unit	QWR	HWR	SSR1	SSR2
Frequency	MHz	81.25	162.5	352	325
β_g		0.047	0.12	0.30	0.51
Q	10^9	2.1	4.1	9.2	10.5
QR_s	Ω	21	42	98	112
R/Q	Ω	468	310	246	296
E_{acc}	MV/m	5.2	5.9	6.9	8.6
E_{peak}/E_{acc}		5.6	5.0	6.3	7.2
B_{peak}/E_{acc}	mT/(MV/m)	9.3	8.2	6.63	7.2

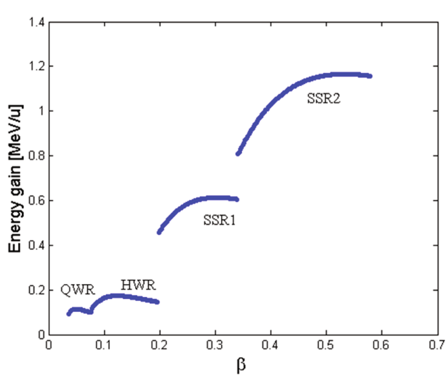

Figure 7: Energy gain in RAON SCL cavities as a function of relativistic β.

Table 4: Cavities and Cryomodules in Driver SCL Linac

	SCL11	SCL12		SCL21	SCL22
Cryomodule #	22	13	19	23	23
Cavity #/CM	1	2	4	3	6
Cavity Type	QWR	HWR	HWR	SSR	SSR

The RAON superconducting linac adopts a double lattice structure with normal conducting magnets. Hence only one QWR cavity is installed in the cryomodule for reducing beam loss generated by machine imperfection. In order to avoid an envelope instability and a parametric resonance through the superconducting linac, transverse and longitudinal phase advances are set under 90 degrees and their ratios are kept about 0.8 expect small region for beam matching. For large beam acceptance, the synchronous phases of SCL cavities are ramping from lower values. The TRACK simulation result of SCL1 and SCL2 is given in Fig. 8 [8]. The rms beam size is less than 3 mm through the superconducting linac. The normalized rms emittance growth is given in Fig. 9 [8]. The transverse emttance growth is negligible and the longitudinal emttance growth is not so large.

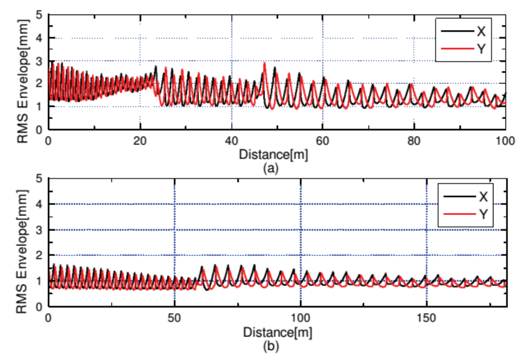

Figure 8: RMS beam envelope in RAON driver linac: (a) SCL1 and (b) SCL2.

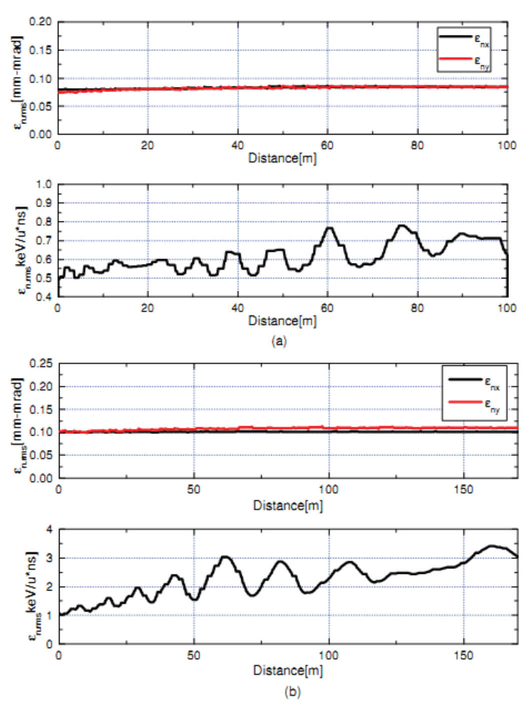

Figure 9: RMS emittance growth in the driver linac: (a) SCL1 and (b) SCL2.

ISBN 978-3-95450-173-1

The final energy of some stables ions are given in Fig. 10 at the driver linac [8].

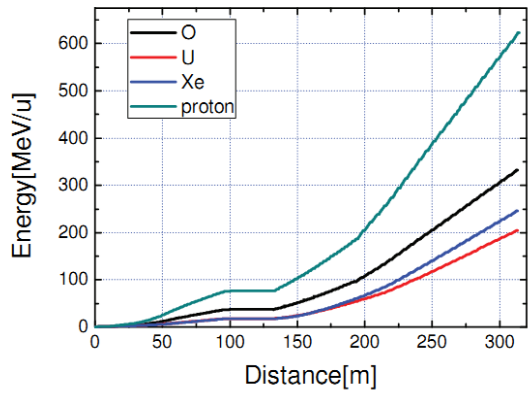

Figure 10: Final energy of stable ions in driver linac.

We used the 2nd order achromat theory [9] in the design of CSS region in order to select 5 charge states of uranium beams and reduce their emittance growth. The TRACK simulation result is given in Fig. 11 and the particle distribution in horizontal phase space at the center of the bending section is given in Fig. 12.

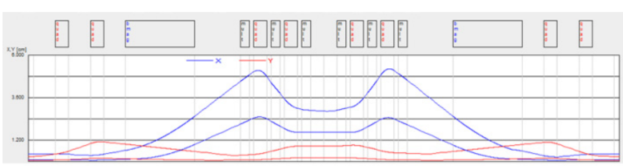

Figure 11: RMS and maximum beam envelope in charge selection section of the driver linac.

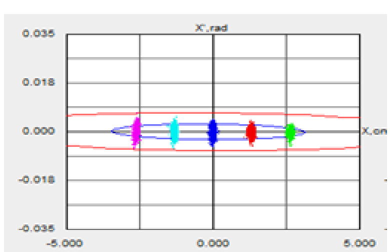

Figure 12: Particle distribution of 5 charge states at the center of charge selection section of the driver linac.

The effects of machine imperfection on beam transmission were studied [10]. The values of misalignment, amplitude and phase errors are summarized in Table 5. The result is given in Fig. 13. The upper plot of the figure shows the beam loss in unit of W/m. The loss is less than 1 W/m even without the orbit correction. The region with the beam loss higher than 1 W/m is the charge stripper region. The lower plot shows the beam center deviation under the machine imperfection.

The fabrication of the prototype SCL cavities is finished as shown in Fig. 14 and their vertical tests are in progress. The prototype cryomodules are under construction in domestic companies as shown in Fig. 15.

Table 5: Machine Imperfection of the Lattice in the RAON Driver Superconducting Linac

Parameters	**Quadrupole**	**Cavities**
Displacement [mm]	±0.15	±1.0
Rotation [mrad]	±5	±5
Amplitude or field [%]	±1	±1
Phase [deg]		±1

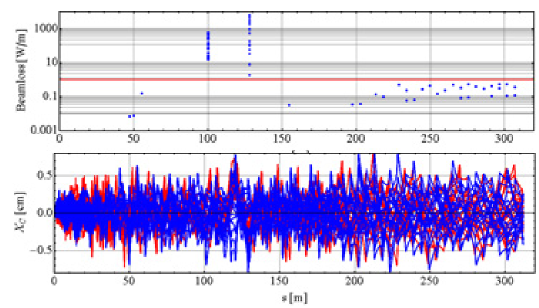

Figure 13: Beam loss and deviation of beam center due to machine imperfection.

Figure 14: Prototype of the SCL cavities: QWR(left), HWR (middle), SSR (right).

Figure 15: The prototype cryomodule for QWR (left) and HWR (right) cavities .

ISBN 978-3-95450-173-1

POST ACCELERATOR

The post accelerator consists of an post injector and another superconducting linac, SCL3 [1]. The injector includes an 18 GHz ECR ion source, an LEBT, a 400 keV/u RFQ, and a MEBT. The ECR ion source will be used in the beam commissioning and test of the post accelerator. The LEBT matches RI beams from ISOL system into the post RFQ. The reference particle of RI beams is ^{132}Sn with A/q of about 8 which are generated by charge breeders in the ISOL facility. The input beam energy of the RFQ is 5keV/u and the output energy is 400 keV/u. The post MEBT includes 6 quadrupole magnets and 2 buncher cavities for beam manipulation in transverse and longitudinal directions, respectively.

The SCL3 uses the same type of QWR and HWR cavities as in the SCL1 and the lattice structure is also doublet as the SCL1 [1,8]. Fig. 16 shows the rms beam envelope in SCL3. It is less than 3 mm in almost all region of SCL3.

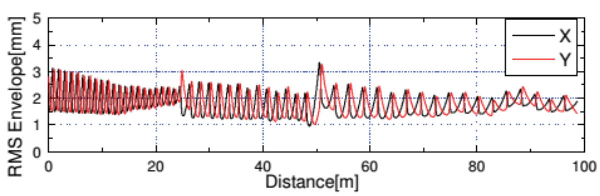

Figure 16: RMS envelope in SCL3.

The P2DT is a beam transport line between SCL3 and SCL2 for further acceleration of the RI beams. There is a charge stripper at the entrance of P2DT line and it makes Sn beams of the single charge state to 3 charge states, 45, 46 and 47. The bending angle of P2DT line is 180 degrees as shown in Fig 1. It is separated into two 90-degree bending sections. Each bending sections satisfies the 2nd order achromatic condition. TRACK simulation result is given in Fig. 17 through 180 degree bending section. The particle distribution in horizontal phase space at the center of the first 90-degree bending section is given in Fig. 18.

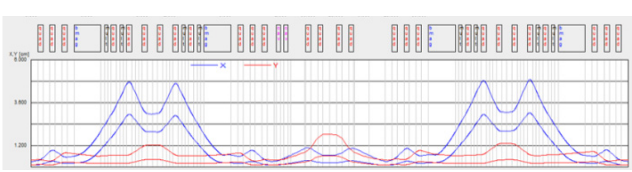

Figure 17: Beam envelope in P2DT line.

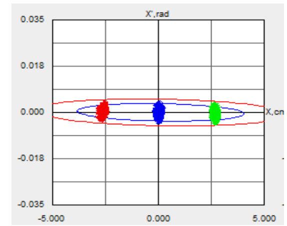

Figure 18: Particle distribution of 3 charge states at the center of the first 90-degree bending section in P2DT.

CONCLUSION

This work summarized the beam dynamics design and the status of development of critical components in the RAON linac facilities. The optimization study of beam dynamics is in progress. The development of prototype ECR ion source and RFQ is finished. The low temperature test of the assembled superconducting magnets in the ion source and the RF test of the prototype RFQ of one section will be finished in near future. The prototype cavities for RAON SCL have been fabricated and their vertical tests are in progress. The fabrication of the cryomodules is almost finished.

REFERENCES

[1] D. Jeon et al, J. Korean Phys. Soc. 65, 1010 (2014).
[2] D. Jeon and H.J. Kim, "Staus of the RAON Heavy Ion Accelerator Project", WEIOB03, LINAC 2014, Geneva, Switzerland (2014).
[3] I.S Hong et al, Rev. Sci. Instrum. 85, 02A709 (2014).
[4] P.N. Ostroumov, V.N. Aseev and B. Mustapha, TRACK, ANL Technical Note, Updated for version 3.7.
[5] K.R. Crandall et al, RFQ Design Codes, LA-UR-96-1839.
[6] H.J. Kim, et al, J. Korean Phys. Soc. 65, 1249 (2014).
[7] H.J. Kim et al, "Superconducting Linac for RISP", MOPP082, LINAC 2014, Geneva, Switzerland (2014).
[8] H.J. Jang et al, "Beam Dynamics Study for RAON Superconducting", MOPP080, LINAC 2014, Geneva, Switzerland (2014).
[9] K. L. Brown, "A Second-order Magnetic Optical Achromat", IEEE translation on Nuclear Physics, NS-26, p. 3490, June 1979.
[10] J.K. Hwang et al, "Estimation and Correction of the Uncontrolled Beam Loss due to the Alignment Error in the Low-Energy Linear Accelerator of RAON", May 2013, IPAC 2013, p. 2570 (2014) ; http://www.JACoW.org

ISBN 978-3-95450-173-1